kinetic curve for the 2,3-pyridinedicarboxylato complex indicated the formation and decay of an intermediate species; with (Cr^{III}) = 0.004 M and (U^{III}) = 0.0025 M, this intermediate attained its maximum concentration about 8 ms after mixing. Action of U(III) on the 2,3-pyrazinedicarboxylato complex yielded a strongly absorbing yellow-green species, the rate of formation of which was too great to be measured by our methods.

(15) J. A. Laswick and R. A. Plane, *J. Am. Chem. Soc.*, **81**, 3564 (1959).
(16) D. C. Stewart, Argonne National Laboratory Report No. ANL-4812, 1952, p 14.
(17) E. S. Gould, *J. Am. Chem. Soc.*, **87**, 4730 (1965); **88**, 2983 (1966).
(18) Confirmatory evidence on this point arises from recent measurements by J. C.-K. Heh (Kent State University, 1977). The specific rate of reduction (25 °C, μ = 1.2), using Cr^{2+}, of the 2-coordinated monoester complex V has been found to be $500/(H^+)$ M^{-1} s^{-1}, whereas the corresponding (almost acid-independent) specific rate for its 3-coordinated isomer, VI, is 0.5 M^{-1} s^{-1}. Note that the chromium(III) derivative of

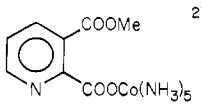

V

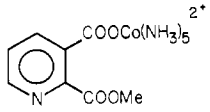

VI

$k_{Cr} = 5 \times 10^2/(H^+)$ M^{-1} s^{-1} $k_{Cr} = 0.5$ M^{-1} s^{-1}

2,3-pyridinedicarboxylic acid in the present series reacts considerably more rapidly with Cr^{2+} than does the 3-coordinated cobalt(III) complex, VI.

(19) A. Haim and N. Sutin, *J. Am. Chem. Soc.*, **88**, 434 (1966), report a specific rate greater than 2×10^4 M^{-1} s^{-1} for the reaction $Cr(SCN)OH^+ + Cr^{2+} \rightarrow Cr^{2+} + Cr(NCS)OH^+$.
(20) In view of evidence that pyridinecarboxylic acids exist predominantly in their zwitterionic forms in aqueous solution (see, for example, R. W. Green and K. H. Tong, *J. Am. Chem. Soc.*, **78**, 4896 (1956)), a large fraction of the deprotonated form of I would be expected to be microspecies VII. Since the observed specific rate for reduction of two rapidly equilibrating species is the weighted average of the individual specific rates, the specific rate associated with VIII alone would be considerably greater than 10^3 M^{-1} s^{-1}.
(21) In their study of the Cr^{2+} reduction of the maleato derivative of $(NH_3)_5Co^{III}$, M. V. Olson and H. Taube, *Inorg. Chem.*, **9** 2072 (1970), extend their measurements to (H^+) = 0.004 M, at which acidity about 30% of the maleato complex (K_a = 0.00182) is converted to its conjugate base. Since k_{Cr} for this complex neither increases nor decreases with acidity in the range 0.004–1.0 M, it must be inferred that, in this one case, the protonated and nonprotonated forms of the oxidant are reduced at very nearly the same specific rate.
(22) (a) J. C. Chen and E. S. Gould, *J. Am. Chem. Soc.*, **95**, 5539 (1973); (b) F.-R. F. Fan and E. S. Gould, *Inorg. Chem.*, **13**, 2639 (1974); (c) A. H. Martin and E. S. Gould, *ibid.*, **14**, 873 (1975).
(23) Although we have not attempted to identify the products formed from reductions of the ligands, analogy with a related system[24] suggests formation of the bimolecular reduction product IX in the pyruvato reactions

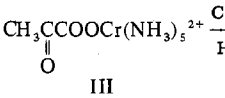

III

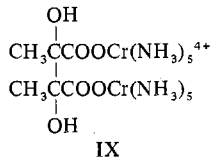

IX

Moreover, in view of the very rapid dimerization reported for a large number of related one-electron reduction products in aqueous media,[25] it seems likely that bimolecular chromium(III) products are formed also in the reductions by U^{3+} in the present study.

(24) E. S. Gould, N. A. Johnson, and R. B. Morland, *Inorg. Chem.*, **15**, 1929 (1976).
(25) See, for example: (a) H. Cohen and D. Meyerstein, *Isr. J. Chem.*, **12**, 1049 (1974); (b) M. Simic, P. Neta, and E. Hayon, *J. Phys. Chem.*, **73**, 3794 (1969); (c) E. Hayon, T. Ibata, N. Lichtin, and M. Simic, *ibid*, **76**, 2072 (1972).
(26) For descriptions of radical intermediates in related systems, see: (a) M. Z. Hoffmann and M. Simic, *J. Am. Chem. Soc.*, **94**, 1757 (1972); (b) E. S. Gould, *ibid.*, **94**, 4360 (1972).
(27) A reviewer has asked whether it is reasonable to attribute the observed differences in the behavior of Cr^{2+} and U^{3+} to the action of the latter as a two- rather than a one-electron reductant. In view of the marked instability of the two-electron oxidation product, U(V), under our reaction conditions[28] and in view of the difficulty in carrying out one-electron oxidations of U(IV) in oxidizing media similar to ours,[29] we consider this alternative as relatively unlikely.

(28) L. B. Asprey and B. B. Cunningham, *Prog. Inorg. Chem.*, **2**, 290 (1960).
(29) See, for example, R. T. Wang and J. H. Espenson, *J. Am. Chem. Soc.*, **93**, 380 (1971).

Contribution from the School of Chemical Sciences, University of Illinois, Urbana, Illinois 61801

Magnetic Exchange Interactions in Transition-Metal Dimers. 14. Binuclear Copper(II) Schiff Base Compounds of Salicylaldehyde with Aromatic Polyamines[1]

ELVIRA F. HASTY, LON J. WILSON, and DAVID N. HENDRICKSON*[2,3]

Received July 13, 1977

The variable-temperature (4.2–290 K) magnetic susceptibility characteristics of three binuclear copper(II) complexes, two binuclear nickel(II) complexes, and one binuclear cobalt(II) complex are reported. Each binuclear complex has an iminobenzene moiety bridging between the two metal ions. Condensation of salicylaldehyde with either *m*- or *p*-phenylenediamine gives ligands which react with cupric ion to give the complexes Cu_2(sal-*m*-pda)$_2$ and Cu(sal-*p*-pda)$_2$, respectively. The magnetism of the former is found to be as reported previously. An improved glass EPR spectrum is reported which shows *intra*dimer zero-field splitting. The compound Cu_2(sal-*p*-pda)$_2$ has an antiferromagnetic interaction ($J \simeq -1.9$ cm^{-1}) of essentially comparable strength to Cu_2(sal-*m*-pda)$_2$. The compound Ni_2(sal-*m*-pda)$_2 \cdot 3H_2O$ also shows an antiferromagnetic interaction with $J = -1.6$ cm^{-1}. Condensation of 2,2′,6,6′-tetraaminobiphenyl with salicylaldehyde gives a binucleating ligand which is used to prepare Cu_2(sal-tabp), Ni_2(sal-tabp)$\cdot H_2O$, and Co_2(sal-tabp)$\cdot {}^1/_2H_2O$. The copper(II) compound shows very little sign of an interaction in the susceptibility data taken down to 4.2 K. The room temperature $CHCl_3$ solution EPR spectrum, however, shows that there is an interaction. The liquid nitrogen temperature $CHCl_3$ glass EPR spectrum is well resolved for Cu_2(sal-tabp). Some comments and data are presented bearing on the electrochemistry of binuclear copper(II) complexes. Both Ni_2(sal-tabp)$\cdot H_2O$ and Co_2(sal-tabp)$\cdot {}^1/_2H_2O$ show weak antiferromagnetic exchange interactions in their susceptibility curves to 4.2 K, which are fit to give $J = -0.49$ and $J = -0.60$ cm^{-1}, respectively.

Introduction

In previous work[4] the magnetic exchange interactions present in the binucleated copper(II) complexes $Cu_2A^4(B^3)_2$ and $Cu_2A^3(B^3)_2$ were determined. An *intra*molecular antiferromagnetic exchange interaction was found to be present in $Cu_2A^4(B^3)_2$ where $J = -12$ cm^{-1} (Hamiltonian = $-2J\hat{S}_1 \cdot \hat{S}_2$). The interaction between the two copper(II) ions, which are separated by ca. 7.5 Å, is propagated by the 1,2,4,5-tetra-

0020-1669/78/1317-1834$01.00/0

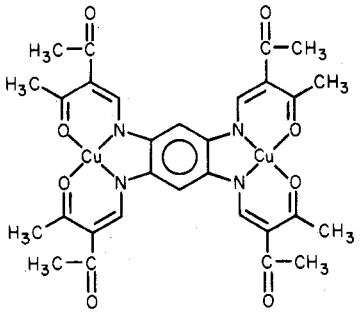

$Cu_2A^4(B^3)_2$

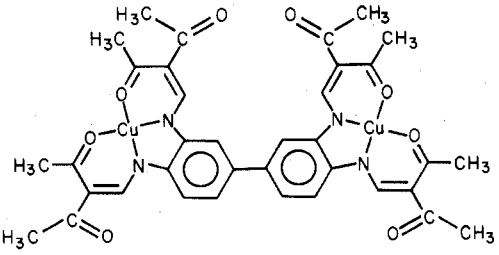

$Cu_2A^3(B^3)_2$

iminobenzene moiety. No indication of an exchange interaction was detected in the magnetic susceptibility taken down to 4.2 K for $Cu_2A^3(B^3)_2$. This work led to an investigation of the facility of other polyaminobenzene moieties to provide viable bridges for magnetic exchange interactions.

In this paper, we report results for the following six compounds: M_2(sal-*m*-pda)$_2$, I (M = Cu) and II (M = Ni); M_2(sal-*p*-pda)$_2$, III (M = Cu); M_2(sal-tabp), IV (M = Cu), V (M = Ni), and VI (M = Co). The ligands result from the condensation of salicylaldehyde with various aromatic amines:

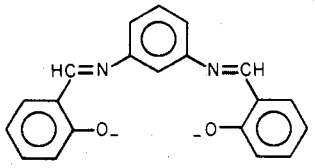

sal-*m*-pda^{2-}

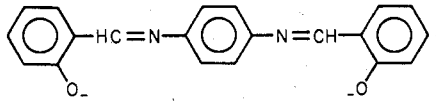

sal-*p*-pda^{2-}

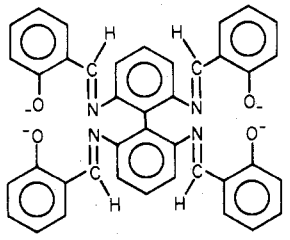

sal-tabp^{4-}

Patterson and Holm[5] studied the electrochemistry of Cu_2(sal-tabp) and a salicylaldehyde substituted derivative of Cu_2(sal-*m*-pda)$_2$. The latter molecule showed only one two-electron reduction wave while Cu_2(sal-tabp) exhibited two one-electron reduction waves. In this paper, we present electrochemical data for $Cu_2A^4(B^3)_2$ and $Cu_2A^3(B^3)^2$ and a simplified analysis of the relationship between magnetic exchange interactions and successive one-electron reduction waves for such binuclear copper complexes.

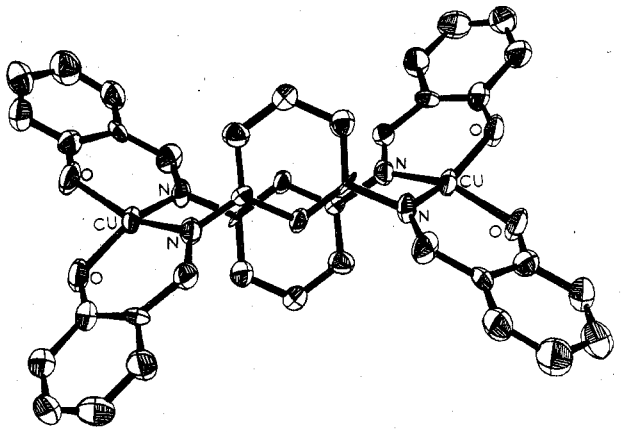

Figure 1. ORTEP plotting of Cu_2(sal-*m*-pda)$_2$. The positional parameters were taken from ref 6.

Results and Discussion

Samples of compounds I–VI were prepared by first condensing the appropriate polyamine with salicylaldehyde and then reacting a solution of the resultant Schiff base ligand with a solution of copper(II), nickel(II), or cobalt(II). Analytical data for all compounds are presented in Table I.

Cu_2(sal-*m*-pda)$_2$. In 1936, Pfeiffer and Pfitzner[6] condensed salicylaldehyde with either *m*-phenylenediamine or *p*-phenylenediamine; Cu(II) and Ni(II) complexes were formed with the ligand resulting from the meta compound, while only a Cu(II) complex was prepared with the para isomer. The Cu(II) and Ni(II) complexes of the meta isomer ligand were formulated as dimers wherein two phenylenediamine moieties are functioning as bridging groups. The dimeric nature was verified for the Cu(II) complex by a recent x-ray structure report.[7] In the following discussion the meta copper compound will be designated as Cu_2(sal-*m*-pda)$_2$, where sal = salicylaldehyde and *m*-pda = *m*-phenylenediamine. The molecular structure of Cu_2(sal-*m*-pda)$_2$ is depicted in Figure 1. The coordination geometry at each copper ion is almost midway between cis-planar and tetrahedral.

Jeter and Hatfield[8] studied the variable-temperature magnetic susceptibility and EPR characteristics of Cu_2(sal-*m*-pda)$_2$. The magnetic susceptibility data (2.7–290.0 K) fit the Curie–Weiss law, $\chi = C/(T + \Theta)$, with $C = 0.374$ and $\Theta = -0.5$ K. In addition, their data were fitted to the Van Vleck dimer exchange interaction equation[9]

$$\chi = \frac{g^2\beta^2N}{3kT}\,[1 + {}^1/_3 \exp(-2J/kT)]^{-1} + N\alpha$$

to give $J \simeq -0.5$ cm^{-1}, where $2J$ is the energy separation between the singlet and triplet spin states. EPR data were also presented for Cu_2(sal-*m*-pda)$_2$. Their X-band EPR spectrum for the pure powdered solid exhibited a very strong unsymmetrical absorption near 3200 G with weak bands at ~1500, 4700, and 6100 G, while their X-band spectrum for a $CHCl_3$ liquid nitrogen temperature glass showed seven main absorptions. Two of the seven main absorptions (3090 and 3120 G) were attributed to impurities with the spin states $S = {}^1/_2$. Jeter and Hatfield[8] analyzed their spectrum to give $g_\parallel = 2.18$, $g_\perp = 2.09$, and $|D| = 0.022$ cm^{-1} with the assumption that the nonaxial zero-field parameter, E, is negligible. The two high-field weak features (4700 and 6100 G) in the pure sample spectrum were tentatively assigned as the parallel and perpendicular components of a singlet ($S' = 0$, $M_s = 0$) to triplet ($S' = 1$, $M_s = +1$) transition.

We have prepared a crystalline analytically pure (see Table I) sample of Cu_2(sal-*m*-pda)$_2$ as a chloroform solvate. The magnetic susceptibility characteristics of our sample were found to be essentially identical. However, improved EPR results were obtained. The X-band EPR powder spectrum

Table I. Analytical Data

Compound	%C		%H		%N		%M	
	Calcd	Obsd	Calcd	Obsd	Calcd	Obsd	Calcd	Obsd
Cu_2(sal-*m*-pda)·2$CHCl_3$	50.72	51.00	3.05	3.13	5.63	5.72	12.78	12.50
Cu_2(sal-*p*-pda)·$^1/_2CHCl_3$	59.65	60.24	3.53	3.70	6.87	6.61	15.58	15.72
Cu_2(sal-tabp)	63.72	63.70	3.47	3.63	7.43	7.52	16.86	16.47
Ni_2(sal-*m*-pda)$_2$·3H_2O	60.03	60.31	4.29	4.32	7.00	6.81	14.67	14.30
Ni_2(sal-tabp)·H_2O	62.94	62.69	3.70	3.65	7.35	7.41	15.40	15.25
Co_2(sal-tabp)·$^1/_2H_2O$	63.88	63.69	3.62	3.55	7.45	7.71	15.68	15.55

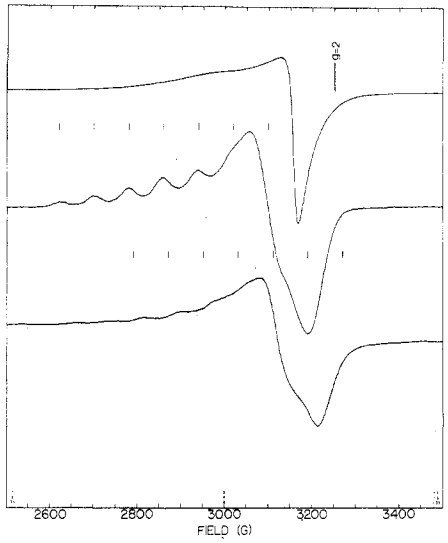

Figure 2. X-Band (ca. 9 GHz) EPR spectra of Cu_2(sal-*m*-pda)$_2$: top, powdered solid sample; middle, DMF glass at liquid-nitrogen temperature; bottom, $CHCl_3$ glass at liquid-nitrogen temperature, obtained as a CAT of 30 5-min scans.

(both room temperature and 77 K) of our sample (see Figure 2) showed a very strong absorption at ~3200 G and a weak absorption at ~1500 G; there were *no* weak absorptions at 4700 and 6100 G as reported by Jeter and Hatfield.[8] We concur that the weak absorption at ~1500 G can be assigned to a $\Delta M_s = 2$ transition for the Cu(II) dimer. Contrary to their findings, the parallel ($g_\parallel = 2.194$) and perpendicular ($g_\perp = 2.063$) $\Delta M_s = 1$ signals are readily discernible in our powder spectrum as can be seen in Figure 2 (top). Additional differences become apparent as we turn to the spectra of "magnetically diluted" samples.

A 77 K dimethylformamide (DMF) glass spectrum was obtained for our sample of Cu_2(sal-*m*-pda)$_2$ and it is reproduced in Figure 2 (middle). Six peaks can be seen in the DMF glass spectrum to the low-field side of the "perpendicular region"; the separation between the six peaks is ~80 G. The magnetic susceptibility curve and the $\Delta M_s = 2$ ESR transition indicate the presence of an intramolecular electron exchange in Cu_2(sal-*m*-pda)$_2$. In the simple case, 14 lines, that is, two sets (due to zero-field splitting) of seven copper hyperfine lines would be expected[10] in the parallel signal for such a copper dimer. It is apparent that the two sets of seven lines overlap, leading to the appearance of fewer than 14 lines. It is also evident from Figure 2 (middle) that the two large impurity peaks reported by Jeter and Hatfield (for a $CHCl_3$ glass spectrum) are *not* present in our DMF glass spectrum and as such an analysis is seemingly more straightforward. In the parallel signal of this DMF glass spectrum, two sets, each having seven peaks, can be tentatively identified as indicated in Figure 2. The highest field peak of the high field set of seven peaks is not readily visible perhaps due to low intensity and/or overlapping with the perpendicular signal. It is important to note that this assignment gives $A_\parallel \simeq 80$ G, which is as expected (half of monomer value) for a copper dimer with magnetic exchange. In addition, because the spacing between the two seven-peak parallel signals is $2D_\parallel$, this assignment gives $D_\parallel \simeq 80$ G. Jeter and Hatfield approximated the Cu–Cu distance in Cu_2(sal-*m*-pda)$_2$ as 8.5 Å from the X-ray structure. Using the computer program JAM and the X-ray structural results, we find that the Cu–Cu distance is, in fact, 7.44 Å. Since there is probably very little pseudo-dipolar interaction in this dimer, the dipolar zero-field interaction can be calculated from the following equation:[11]

$$D_{dd}(\parallel) = 0.65 g_\parallel^2 / R^3$$

In Cu_2(sal-*m*-pda)$_2$, the Cu–Cu distance R is 7.44 Å and $g_\parallel = 2.20$, which gives $D_{dd}(\parallel) = 0.0076$ cm^{-1} = 82 G. This agrees with $D_\parallel$ from the above assignment. The $D_\parallel = 0.022$ cm^{-1} value obtained by Jeter and Hatfield is considerably too large for the R value corresponding to Cu_2(sal-*m*-pda)$_2$, if the above equation is applicable.[12]

The question that remains is why there is such a difference between our DMF glass spectrum and the $CHCl_3$ glass spectrum obtained by Jeter and Hatfield. There could be a difference in the impurity level in the two samples, or perhaps dissolution in $CHCl_3$ leads to some decomposition. Another explanation for the difference in appearance of the DMF vs. $CHCl_3$ glass spectra lies in a possible difference in geometry of the dimer in the two media. The work of Smith and Pilbrow[13] has shown that even for copper dimers with centers of symmetry, as is present for the Cu_2(sal-*m*-pda)$_2$ in the solid, complicated EPR spectra result if the **D** and **g** tensors are misaligned. In DMF, the solvent could be coordinating with the copper in Cu_2(sal-*m*-pda)$_2$, resulting in a dimer configuration where there is little misalignment between the **D** and **g** tensors. Chloroform would not coordinate to the copper ion and the $CHCl_3$ solution structure of Cu_2(sal-*m*-pda)$_2$ would probably approximate that found for the solid.

We have studied the stability of Cu_2(sal-*m*-pda)$_2$ dissolved in either DMF or $CHCl_3$ using a UV–visible spectrophotometer and found that there is *no* change in the spectrum for either solution for a period of 1 day. Thus, barring immediate decomposition upon dissolution, it does not appear that the difference in EPR glass spectra (our DMF vs. the reported $CHCl_3$) can be attributed to decomposition in either solvent. We found the solubility of Cu_2(sal-*m*-pda)$_2$ to be lower in $CHCl_3$ (so low that osmometry measurements could not be done) than in DMF and, as a consequence, our 77 K $CHCl_3$ spectrum was found to be of lower quality than the DMF spectrum. It was possible, however, to obtain a reasonable quality computer-averaged transient (CAT of 30 5-min scans) 77 K $CHCl_3$ glass spectrum which is shown in the bottom tracing in Figure 2. Contrary to the reported spectrum of Jeter and Hatfield, our CAT chloroform glass spectrum is similar to the DMF glass spectrum. Furthermore, we have obtained similar but lower resolution spectra for dimethyl sulfoxide and pyridine glasses of Cu_2(sal-*m*-pda)$_2$.

In summary, a good resolution EPR spectrum of Cu_2(sal-*m*-pda)$_2$ is difficult to obtain because of low solubility. The D value reported by Jeter and Hatfield does *not* seem to be appropriate for the Cu–Cu distance in Cu_2(sal-*m*-pda)$_2$. Most important to this work, however, is the observation that

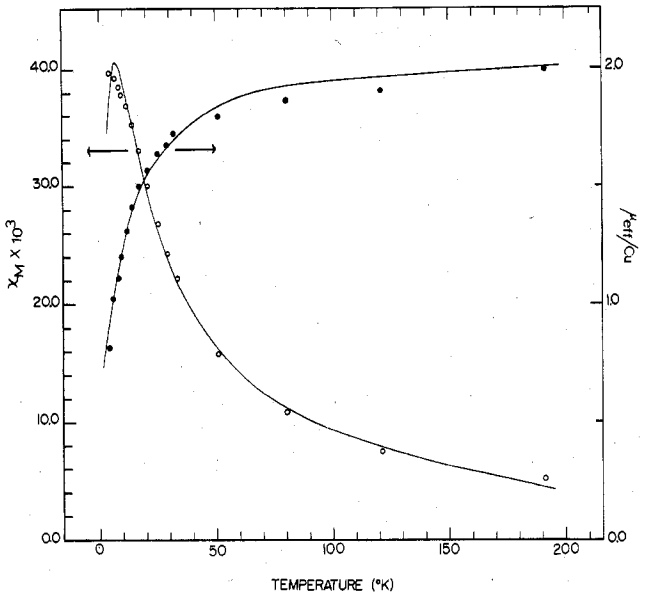

Figure 3. Experimental molar paramagnetic susceptibility (○) per dimer and effective magnetic moment (●) per Cu(II) ion vs. temperature curves for Cu_2(sal-*p*-pda)$_2$·$^1/_2CHCl_3$. The solid lines represent the least-squares fit to the theoretical equation; see text.

Cu_2(sal-*m*-pda)$_2$ has an antiferromagnetic exchange interaction with $J \simeq -0.5$ cm^{-1}.

Cu_2(sal-*p*-pda)$_2$. The compound Cu_2(sal-*p*-pda)$_2$, as a chloroform solvate, was found to be relatively insoluble in comparison to the meta analogue. The slight solubility of this para compound in $CHCl_3$ and CH_2Cl_2 precluded the determination of an effective molecular weight. Pfeiffer and Pfitzner[6] concluded that Cu_2(sal-*p*-pda)$_2$ is polymeric.

Variable-temperature (4.2–290 K) magnetic susceptibility data were collected for the para compound; the data are given in Table II[14] and illustrated in Figure 3. The data were fitted with a modification of the above Bleaney–Bowers equation where T is replaced by $T - \Theta$: the least-squares fit is given as a solid line in Figure 3. *Inter*molecular interactions can be gauged[15] by Θ, the Curie–Weiss constant. The temperature-independent paramagnetism ($N\alpha$) was taken (as it was above) as 120×10^{-6} cgsu/mol of dimer. The best fit parameters were found to be $J = -1.9$ cm^{-1}, $\Theta = 13.3$ K, and $g = 2.38$. The g value from this fitting is undoubtedly too large, a fact that will be evident from the EPR of this compound, to which we turn.

A broad slightly asymmetric peak at 3070 G ($g = 2.11$) is seen in the X-band powder spectrum of Cu_2(sal-*p*-pda)$_2$. The low solubility of this compound led to 77 K glass spectra of such a low quality as to be useless. The parallel and perpendicular signals are resolved in the Q-band powder spectrum to give $g_\parallel = 2.190$ and $g_\perp = 2.093$. In both cases a weak and broad half-field ($g = 3.72$) transition is seen and, if this compound is indeed dimeric, not polymeric, this signal could be assigned to a $\Delta M_s = 2$ transition. Thus, the magnetism and EPR point to the presence of an exchange interaction; however, it is difficult to decide whether the compound is dimeric or polymeric. A crystal structure is needed.

Cu_2(sal-tabp)$_2$. The binucleating ligand tabp, formed by the condensation of salicylaldehyde and 2,2′,6,6′-tetraaminobiphenyl, reacts with cupric ion to give Cu_2(sal-tabp). In the following, it will be shown that there is a weak *intra*molecular exchange interaction present in this compound. The dimeric nature of this compound was verified by the observation in the mass spectrum of a relatively intense cluster of four peaks located about a m/e value of 753 and by molecular weight measurements in CH_2Cl_2 giving an effective molecular weight of 768. The molecular weight of Cu_2(sal-tapb) is calculated to be 753. Apparent structural similarities between Cu_2(sal-tabp) and Cu_2(sal-*m*-pda)$_2$ are evident. However, it is clear that the "additional" bond between the *m*-diimino moieties in Cu_2(sal-tabp) could impose different coordination geometries about the copper atoms.

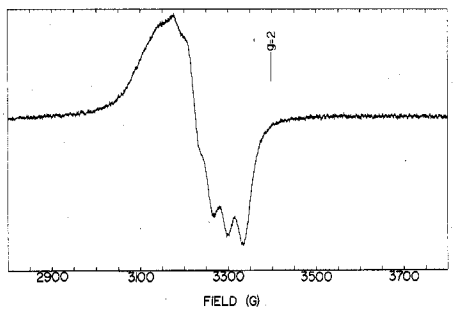

Figure 4. X-Band EPR spectrum of a room-temperature $CHCl_3$ solution of Cu_2(sal-tabp).

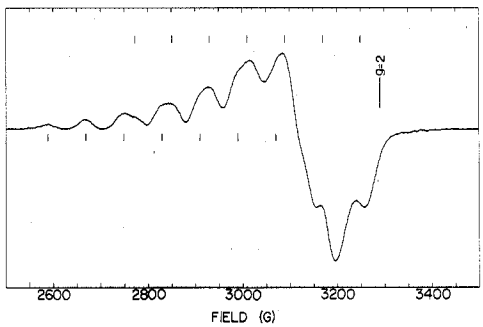

Figure 5. X-Band EPR spectrum of a liquid nitrogen temperature $CHCl_3$ glass of Cu_2(sal-tabp).

The X-band EPR spectrum of a powdered sample of Cu_2(sal-tabp) shows an intese absorption at 3070 G and a very weak absorption at 1550 G ($g = 4.20$), the latter being assigned to a $\Delta M_s = 2$ transition. The parallel and perpendicular signals are not resolved at X-band frequencies; however, the Q-band powder spectrum clearly resolves both signals, the parallel at 11 220 G ($g_\parallel = 2.233$) and the perpendicular at 12 040 G ($g_\perp = 2.080$).

Very pleasing X-band spectra were obtained for Cu_2(sal-tapb), both in a room-temperature $CHCl_3$ solution and in a liquid-nitrogen $CHCl_3$ glass. Reproductions of both spectra are given in Figures 4 and 5. Seven copper hyperfine lines are evident in the room-temperature spectrum, showing that there is an *intra*molecular exchange interaction in Cu_2(sal-tabp). This is one of the few binuclear copper molecules that stays intact in solution. In the room-temperature spectrum, there are only 7 hyperfine lines instead of 14, because the tumbling of the binuclear copper molecule averages to zero any zero-field interaction between the copper atoms. From the spacing in this spectrum, A_{av}(Cu) is found to be 33 G, and from the center of the spectrum at 3225 G, g_{av} is found to be 2.130.

As can be seen in Figure 5, cooling the $CHCl_3$ solution to liquid-nitrogen temperature to give a glass leads to a more complicated spectrum due to the presence of both $g_\parallel$ and $g_\perp$ signals as well as zero-field splitting. The identification of 14 copper hyperfine lines on the parallel signal is easier for this $CHCl_3$ glass spectrum of Cu_2(sal-tabp) than the DMF glass spectrum of Cu_2(sal-*m*-pda)$_2$ given in Figure 2 (middle). As indicated by the vertical lines in Figure 5, an analysis of the $CHCl_3$ glass spectrum of Cu_2(sal-tabp) gives $A_\parallel \simeq 80$ G and $D_\parallel \simeq 92$ G. In comparison to Cu_2(sal-*m*-dpa)$_2$, the $A_\parallel$ value for Cu_2(sal-tabp) is essentially the same, whereas the $D_\parallel$ value is ~12 G larger. This is not a very large difference, but a larger $D_\parallel$ for Cu_2(sal-tabp) implies a shorter Cu–Cu distance

Table III. Magnetic Data for Cu_2(sal-tabp)[a]

T, K	μ_{eff}/Cu, μ_B	T, K	μ_{eff}/Cu, μ_B
290	1.96	20.5	2.01
255	1.95	17.0	2.04
221	1.96	14.0	2.05
191	1.95	11.7	2.03
121	1.90	9.5	1.95
80.0	1.94	8.0	1.89
64.5	1.96	6.7	1.81
51.0	1.97	5.7	1.77
33.5	2.01	5.0	1.75
29.0	2.01	4.2	1.64
25.0	2.01		

[a] Diamagnetic correction used: -345×10^{-6} cgsu/mol of binuclear complex.

in this molecule, which is in qualitative agreement with what would be expected from the constraining effect associated with the biphenyl bond. Irrespective of the origin of the larger $D_{\|}$ value for Cu_2(sal-tabp), it leads to less accidental overlap of the two zero-field split seven-line patterns. Starting from low field, the third "maximum" shows a marked asymmetry as do some of the yet higher-field maxima. The similarity of assignment of the spectra of Cu_2(sal-*m*-pda)$_2$ and Cu_2(sal-tabp) is substantiation for the correctness of assignment in each case. With $A_{\|}$ and A_{av} from the glass and room-temperature solution spectra, respectively, it is possible to calculate $A_{\perp}$(Cu) $\simeq$ 9.5 G for Cu_2(sal-tabp).

EPR has given a clear indication of the presence of *intra*molecular exchange interactions in Cu_2(sal-tabp) and it is possible to conclude from the EPR data that $|J|$ > ca. 0.02 cm^{-1} for Cu_2(sal-tabp). Magnetic susceptibility data taken down to 4.2 K can set the upper limit for the exchange parameter. Table III summarizes the susceptibility data for Cu_2(sal-tabp). The 290 K μ_{eff} value of 1.96 μ_B stays relatively constant until ~60 K, whereupon there is a small increase with decreasing temperature followed by a drop in μ_{eff} to 1.63 μ_B at 4.2 K. The spin-only value for one unpaired electron is, of course, 1.73 μ_B. The small depression of μ_{eff} below the spin-only value could result from an interaction where $J \approx -0.2$ cm^{-1}. However, a quantitative evaluation of the J value for this compound would require susceptibility data taken to sub-helium temperatures. For our purposes, it is sufficient to know that there is an *intra*molecular exchange interaction in Cu_2(sal-tabp) and that it is weak with ca. 0.02 $cm^{-1} < |J| <$ ca. 0.2 cm^{-1}.

The copper(II) ion coordination geometry in Cu_2(sal-tabp) is probably close to that which has been characterized for the "monomer" analogue of Cu_2(sal-tabp). Lions and Martin[16] reacted cupric ion with the condensation product of salicylaldehyde and 2,2′-diaminobiphenyl to give a copper(II) complex, Cu(sal-dabp). The single-crystal X-ray structure

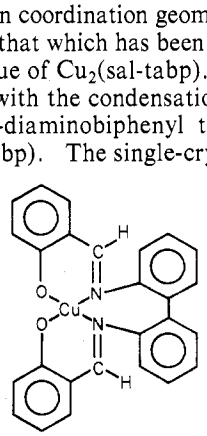

Cu(sal-dabp)

of this compound, *N*,*N*′-(2,2′-biphenyl)bis(salicylaldiminato)copper(II), has been reported.[17] The coordination geometry at the copper(II) ion is intermediate between tetrahedral and square-planar (the workers preferred to describe it as a distorted planar environment). The dihedral angle between the plane defined by the Cu, the N and O of one salicylaldiminato residue and the plane defined by the Cu and the N and O of the other salicylaldiminato residue is 37° instead of the 90° expected for a tetrahedral environment. The dihedral angle between the two rings of the biphenyl group is 57°.

In summary, the local copper(II) ion geometries and magnetic exchange interactions are very similar for Cu_2(sal-tabp) and Cu_2(sal-*m*-pda)$_2$. On the other hand, the magnetic exchange interaction ($J = -12$ cm^{-1}) is somewhat greater in the copper(II) dimer, $Cu_2A^4(B^3)_2$, formed from a binucleating ligand that we previously studied.[4] The copper coordination geometry in $Cu_2A^4(B^3)_2$ is square planar and this probably leads to a greater antiferromagnetic interaction.

Patterson and Holm[5] studied the electrochemistry of Cu_2(sal-tabp) and a salicylaldehyde-substituted derivative of Cu_2(sal-*m*-pda)$_2$. The Cu–Cu distance in the latter compound is 7.44 Å and an ac polarographic study of the derivative showed only one copper reduction wave. The Cu–Cu distance in Cu_2(sal-tabp) is estimated to be ca. 6 Å and in this case ac polarography resolved the peak potentials for two one-electron processes separated by 0.12 V. Thus, Cu_2(sal-tabp) successively adds one electron at a time; reduction of the one copper(II) ion affects the potential at which the second copper(II) ion is reduced. The two waves are resolved only for the binuclear complex with the shorter Cu–Cu distance.

Relative to the observation of successive one-electron reduction waves for binuclear copper(II) complexes, the question arises whether the magnitude of the magnetic exchange interaction between the Cu(II) ions influences the separation between the two one-electron reduction waves. At present there are but a few binuclear copper(II) complexes that do *not* dissociate in solution. The complex $Cu_2A^4(B^3)_2$ does seem to remain intact in Me_2SO as per our EPR doping studies.[4] Because this complex has a large Cu–Cu distance of ca. 7.5 Å and yet has an appreciable exchange interaction with $J = -12$ cm^{-1}, it was of interest to study the electrochemistry of this complex and also the analogous complex $Cu_2A^3(B^3)_2$, which shows no signs of an exchange interaction in the susceptibility data to 4.2 K and also in its doped-sample EPR spectrum.

Dc polarograms were obtained for Me_2SO solutions of $Cu_2A^4(B^3)_2$ and $Cu_2A^3(B^3)_2$, employing tetraethylammonium perchlorate at 5×10^{-2} M as a supporting electrolyte and a dropping mercury electrode. The applied voltage, E, was plotted vs. log $[i/(i_d - i)]$, where i is the current at the voltage E and i_d is the diffusion current. The intercept of this plot gives the half-wave potential, $E_{1/2}$, and the slope is $0.059/n$ with n as the number of electrons. In the case of $Cu_2A^3(B^3)_2$, $E_{1/2}$ was found to be −1.058 V vs. SCE with a slope of 72.4 mV, whereas $Cu_2A^4(B^3)_2$ gave $E_{1/2} = -1.058$ V vs. SCE and a slope of 94 mV. There was no evidence of successive half-waves in either dc polarogram, as expected for the case of two nearby reduction waves.

Cyclic sweep voltammetry was also carried out on the Me_2SO solutions using both the hanging-drop mercury electrode and the Pt electrode. Both of the compounds showed cyclic sweep voltammograms which were characteristic of somewhat irreversible waves where $i_{anodic} \neq i_{cathodic}$. The cyclic sweep for $Cu_2A^4(B^3)_2$ showed two almost resolved peaks in the cathodic scan.

Differential-pulse polarography provides a better resolution of nearby half-waves. Me_2SO solutions of $Cu_2A^4(B^3)_2$ and $Cu_2A^3(B^3)_2$ were studied. Figure 6 illustrates the results. The binucleating ligands $H_4A^3(B^3)_2$ and $H_4A^4(B^3)_2$ showed no waves up to −1.5 V under similar conditions. In Figure 6 it can be seen that $Cu_2A^3(B^3)_2$ shows a symmetric "peak" at −1.045 V which did not change in appearance as the modulation amplitude was changed from 100 to 5 mV. At 100-mV modulation amplitude, $Cu_2A^4(B^3)_2$ showed a broad asymmetric

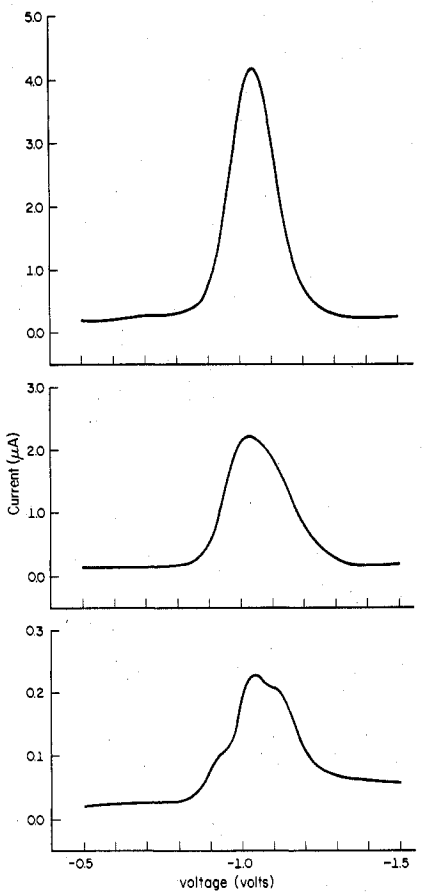

Figure 6. Differential-pulse polarograms of 5×10^{-4} M Me_2SO solutions with 5×10^{-2} M TEAP as electrolyte: top, $Cu_2A^3(B^3)_2$ at a modulation amplitude of 100 mV; middle, $Cu_2A^4(B^3)_2$ at 100 mV amplitude; bottom, $Cu_2A^4(B^3)_2$ at 5 mV amplitude.

peak at −1.060 V. Lowering the modulation amplitude to 5 mV resolved two waves at −1.050 and −1.125 V. The "shoulder" at −0.920 V is attributable to some residual oxygen in the solution. Thus, only $Cu_2A^4(B^3)_2$ shows two successive reduction waves with a separation of ca. 0.08 V. The Cu–Cu distances in $Cu_2A^4(B^3)_2$ and Cu_2(sal-*m*-pda)$_2$ are essentially the same yet the latter does not show two reduction waves. It is interesting that for $Cu_2A^4(B^3)_2$ the J value is −12 cm^{-1}, while for the Cu_2(sal-*m*-pda)$_2$, the J value is only −0.5 cm^{-1}.

A qualitative relationship between the magnitude of ground-state magnetic exchange interaction and separation between the two one-electron reduction waves can be set out for binuclear copper(II) complexes. A molecular orbital approach can be used to assess the antiferromagnetic contribution to a magnetic exchange interaction. In a copper(II) dimer, each copper(II) ion has one unpaired electron in an essentially d-type orbital and, to first order, the antiferromagnetic interaction reflects the level of interaction of the two unpaired-electron orbitals, one located at each copper(II) center. The interaction between the two copper(II) d orbitals is effected by an interaction with the appropriate molecular orbitals of the bridging group. If the two copper(II) ion coordination geometries in a binuclear complex are square planar, then, two molecular orbitals will form as linear combinations of the two $d_{x^2-y^2}$ orbitals.

$$\phi_1 \sim d^a_{x^2-y^2} + d^b_{x^2-y^2}$$

$$\phi_2 \sim d^a_{x^2-y^2} - d^b_{x^2-y^2}$$

As the antiferromagnetic interaction increases, the two molecular orbitals ϕ_1 and ϕ_2 will separate in energy. It has been shown[18-20] that the exchange parameter J for the antiferromagnetic component is given by

$$2J = 2K_{ab} - \frac{2(\epsilon_1 - \epsilon_2)^2}{J_{aa} - J_{ab}}$$

In this expression, J_{ij} and K_{ij} are Coulomb and exchange integrals, respectively, and ϵ_1 and ϵ_2 are the energies of the two orbitals ϕ_1 and ϕ_2, respectively. For closely related binuclear complexes, K_{ij} and J_{ij} would not vary much and, as a consequence it is seen that the exchange parameter is dependent on the energy difference $(\epsilon_1 - \epsilon_2)$.

In the case of a moderately strong ($J < -300$ cm^{-1}) antiferromagnetic interaction, the two formerly unpaired electrons of the two copper(II) ions will be paired up in orbital ϕ_1 at room temperature, viz.

ϕ_2 ——

ϕ_1 ——$\downarrow\uparrow$

There is only a negligible population of the triplet state for the binuclear complex. Thus, for this moderately strongly interacting copper(II) dimer the molecular orbital ϕ_2 is the lowest unoccupied orbital. The first electron taken up in the reduction of the binuclear complex will go into the ϕ_2 orbital. From the above expression for the exchange parameter, it is seen that the binuclear complex with the greater antiferromagnetic interaction has the larger $(\epsilon_2 - \epsilon_1)$ energy difference. As the orbital ϕ_2 is displaced to higher energies with increasing $(\epsilon_2 - \epsilon_1)$ energy difference, it is clear that the first reduction wave will occur at a lower potential. Thus, the binuclear complex with the greatest antiferromagnetic interaction should have the lowest potential first reduction wave. The second electron added to such a binuclear copper(II) complex would also go into the ϕ_2 molecular orbital. The potential for uptake of this second electron will not be the same as for the first electron uptake because of electron–electron repulsion between the two electrons in the ϕ_2 orbital. This electron–electron repulsion should be greatest for the binuclear complex with the greatest antiferromagnetic interaction. Qualitatively, then, binuclear copper(II) complexes with considerable antiferromagnetic interactions should show two successive one-electron reduction waves. Further theoretical and experimental work is needed to quantitatively establish this relationship.

The binuclear copper(II) complexes studied in this work are involved in only weak antiferromagnetic interactions. At room temperature, both the singlet ground state and the triplet excited state are thermally populated for these complexes. The electrochemistry measurements are carried out, of course, at room temperature and as such the electrochemical results for these binuclear complexes reflect the populations of molecules in the triplet and singlet states.

Ni_2(sal-*m*-pda)$_2$·3H_2O and Ni_2(sal-tabp)·H_2O. Variable-temperature magnetic susceptibility data were collected for Ni_2(sal-*m*-pda)$_2$·3H_2O and the results are given in Table IV[14] and Figure 7. As can be seen from the data, this Ni(II) complex is paramagnetic with a μ_{eff} per nickel(II) ion of 3.43 μ_B at 291 K, indicating a high-spin (distorted?) tetrahedral coordination geometry. The effective magnetic moment decreases gradually with decreasing temperature until ca. 50 K below which there is a more pronounced decrease down to 1.72 μ_B per nickel(II) ion at 4.2 K. There is clearly an antiferromagnetic interaction present in Ni_2(sal-*m*-pda)$_2$·3H_2O. If this nickel complex is structurally similar to the copper system, then there are dimeric units. Ginsberg et al.[21] derived the equations for the susceptibility of a nickel(II) dimer treating an isotropic magnetic exchange interaction as well as single-ion zero-field interactions, $D\hat{S}_z^2$, and *inter*dimer interactions with a parameter $Z'J'$. The data for Ni_2(sal-*m*-pda)$_2$·3H_2O were least-squares fit to these equations to give the parameters $J = -1.6$ cm^{-1}, $g = 2.36$, $D = 0.72$ cm^{-1}, and $Z'J' = -1.5°$. The temperature-independent paramagnetism, $N\alpha$, was set equal to 200×10^{-6} cgsu per dimer. In Figure

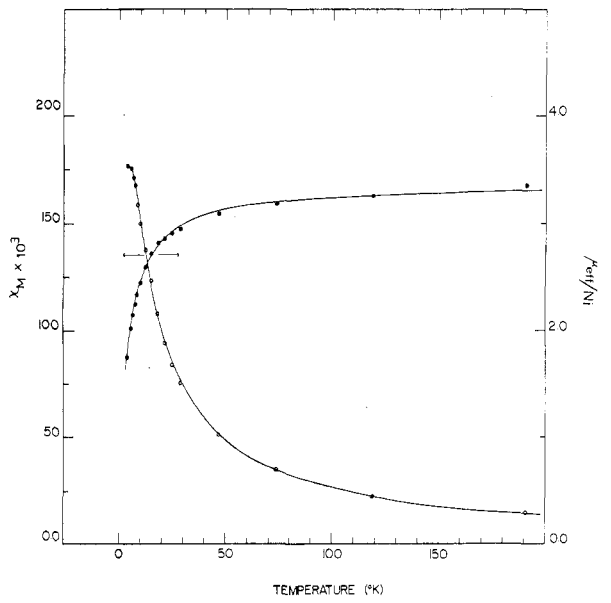

Figure 7. Experimental molar paramagnetic susceptibility (○) per dimer and effective magnetic moment (●) per Ni(II) ion vs. temperature curves for Ni_2(sal-*m*-pda)$_2$·3H_2O. The solid lines represent the least-squares fit to the theoretical equation; see text.

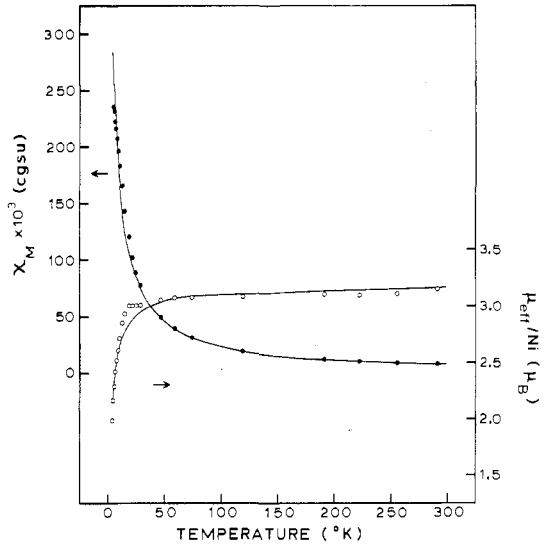

Figure 8. Experimental molar paramagnetic susceptibility (○) per binuclear complex and effective magnetic moment (●) per Ni(II) ion vs. temperature curves for Ni_2(sal-tabp)·H_2O. The solid lines represent the least-squares fit to the theoretical equation; see text.

7, the theoretical fit is given as solid lines which do fit the data very admirably. The good fit can be taken as evidence that this nickel compound is, in fact, dimeric.

Table V[14] and Figure 8 give the magnetic susceptibility data for the other binuclear nickel(II) complex, Ni_2(sal-tabp)·H_2O. In this case, the μ_{eff} per nickel(II) ion at 291 K is 3.15 μ_B, which is appreciably less than the 3.43 μ_B value found for the Ni_2(sal-*m*-pda)$_2$·3H_3O. This could indicate that the coordination geometry is different in the two complexes with the former complex having less of a tetrahedral character. An antiferromagnetic interaction is also evident for Ni_2(sal-tabp)·H_2O with μ_{eff}/Ni at 4.2 K found to be 1.99 μ_B. Least-squares fitting of the data to the equations gives J = −0.49 cm^{-1}, g = 2.22, D = 0.84 cm^{-1}, and $Z'J'$ = −1.2°. Figure 8 shows this fit as solid lines. The fit is not quite as good as for the other nickel compound, but it is still reasonable. The least-squares fitting gives a smaller value of $|J|$ for Ni_2(sal-tabp)·H_2O compared to Ni_2(sal-*m*-pda)$_2$ because the absolute

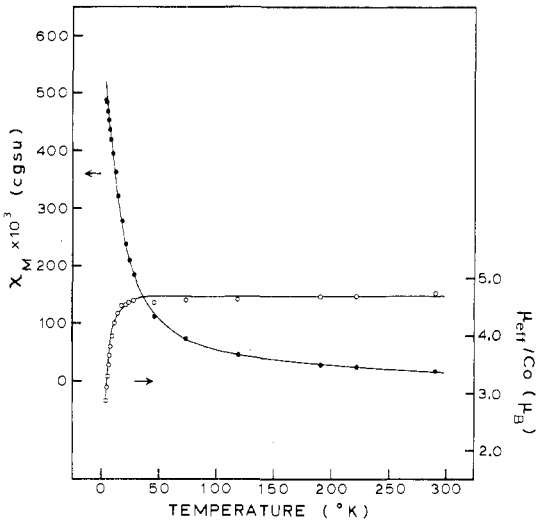

Figure 9. Experimental molar paramagnetic susceptibility (○) per binuclear complex and effective magnetic moment (●) per Ni(II) ion vs. temperature curves for Co_2(sal-tabp)·$^1/_2H_2O$. The solid lines represent the least-squares fit to the theoretical equation; see text.

drop in μ_{eff}/Ni(II) is greater for the latter compound.

Co_2(sal-tabp)·$^1/_2H_2O$. It was relatively easy to prepare the analogous cobalt(II) dimer. Magnetic susceptibility measurements for this compound showed that there is also an antiferromagnetic exchange interaction present. The data are given in Table VI[14] and Figure 9. The μ_{eff}/Co(II) varies from 4.74 μ_B at 291 K to 2.86 μ_B at 4.2 K. Two different theoretical approaches were used to least-squares fit the data. If the temperature dependence of the magnetic susceptibility for a Co(II) dimer is asumed to be due to isotropic magnetic exchange with an assumed isotropic g value and with *inter*dimer exchange interactions accounted for by a Weiss constant, the susceptibility of the Co(II) dimer is given as[22]

$$\chi_M = \frac{2N\beta^2g^2}{kT}\left[\frac{e^{-10x} + 5e^{-6x} + 14}{e^{-12x} + 3e^{-10x} + 5e^{-6x} + 7}\right]$$

where $x = j/kT$. Least-squares fitting to this equation gives J = −0.93 cm^{-1}, g = 2.49, and Θ = −0.11 K.

The other theoretical model employs a spin Hamiltonian for an exchange-interacting high-spin Co(II) dimer including single-ion zero-field splitting, which is given as

$$\mathcal{H} = -2J\hat{S}_1\hat{S}_2 - D(\hat{S}_{1z}^2 + \hat{S}_{2z}^2) - g_i\beta\hat{H}_i\hat{S}_i \qquad i = x, y, z$$

The second term accounts for the single-ion zero-field splitting with the parameter D. The above Hamiltonian matrix is set up with the appropriate coupled basis set and, as detailed previously,[23] the matrix is diagonalized and the magnetic susceptibility is evaluated on each least-squares cycle. It was further assumed that the dimer is axial, i.e., $g_x = g_y = g_\perp$. Least-squares fitting the data for Co_2(sal-tabp)·$^1/_2H_2O$ with this approach gives J = −0.60 cm^{-1}, $g_\parallel$ = 2.60, $g_\perp$ = 2.20, and D = −2.0 cm^{-1}. Figure 9 shows that this fit is quite reasonable.

In short, the antiferromagnetic exchange interaction in Co_2(sal-tabp)·$^1/_2H_2O$ is also very weak as we found for the Ni(II) and Cu(II) analogues. In fact, it is curious that the J values for the three complexes of the composition M_2(sal-tabp)·nH_2O are of such comparable magnitudes. However, it would probably be necessary to ascertain if these three complexes are indeed isostructural before a detailed molecular-orbital based explanation of the similarity of J values could be advanced. In particular, there is a question as to whether in the cases of the Ni(II) and Co(II) complexes the water molecules take up coordination sites.

Experimental Section

Compound Preparation. Analytical data for all compounds appear in Table I. Complexes with the condensation product of phenylenediamine with salicylaldehyde, that is Cu_2(sal-*m*-pda)$_2$, Ni_2(sal-*m*-pda)$_2$, and Cu_2(sal-*p*-pda)$_2$, were prepared according to the procedure reported by Bear et al.[7]

Samples of Cu_2(sal-tabp), Ni_2(sal-tabp)·H_2O, and Co_2(sal-tabp)·$^1/_2H_2O$ were prepared by the following procedure. One millimole of ligand, prepared by the condensation of salicylaldehyde with 2,2′,6,6′-tetraaminobiphenyl,[24] was dissolved in ca. 30 mL of warm absolute methanol. A methanol solution (ca. 25 mL) of 1 mmol of the appropriate $M(OAc)_2 \cdot nH_2O$ salt was added to the ligand solution and the resulting solution was refluxed for 0.5 h and then allowed to cool to room temperature. At this stage of the preparation, a solid had formed in all cases. The solid was collected by filtration and washed with methanol and then diethyl ether. The solids were recrystallized from CH_2Cl_2/Et_2O (1:1 by volume). All solids were dried in vacuo over P_4O_{10} at room temperature for 12 h.

Physical Measurements. EPR and variable-temperature magnetic susceptibility measurements were carried out as described in a previous paper.[25] All EPR samples were loaded into quartz tubes and sealed under vacuum (ca. 10 μ); solutions were degassed prior to sealing the tubes under vacuum. Polarographic measurements were carried out with a Princeton Applied Research Model 174 polarograph. Background corrections were made on all runs and all measurements were made at 25 °C. All solutions were thoroughly bubbled with nitrogen gas before the runs.

Acknowledgment. We are very grateful for support from National Institutes of Health Grant HL 13652 and for computing funds from the University of Illinois Research Board. In addition, L.J.W. thanks the National Institutes of Health for a postdoctoral fellowship (1-F02-AM52131-01).

Registry No. Cu_2(sal-*m*-pda)$_2$, 38651-40-0; Cu_2(sal-*p*-pda)$_2$, 66172-41-6; Cu_2(sal-tabp), 56132-49-1; Ni_2(sal-*m*-pda)$_2$, 66213-50-1; Ni_2(sal-tabp), 66172-42-7; Co_2(sal-tabp), 66172-43-8.

Supplementary Material Available: Tables II, IV, V, and VI, observed and theoretically calculated variable-temperature magnetic susceptibility data for Cu_2(sal-*p*-pda)$_2$, Ni_2(sal-*m*-pda)$_2 \cdot 3H_2O$, Ni_2(sal-tabp)·H_2O, and Co_2(sal-tabp)·$^1/_2H_2O$ (4 pages). Ordering information is given on any current masthead page.

References and Notes

(1) Part 13: E. J. Laskowski and D. N. Hendrickson, *Inorg. Chem.*, **17**, 457 (1978).
(2) Author to whom correspondence should be addressed.
(3) Camille and Henry Dreyfus Teacher–Scholar Fellow, 1972–1977; A. P. Sloan Foundation Fellow, 1976–1978.
(4) E. F. Hasty, T. J. Colburn, and D. N. Hendrickson, *Inorg. Chem.*, **12**, 2414 (1973).
(5) G. S. Patterson and R. H. Holm *Bioinorg. Chem.*, **4**, 257 (1975).
(6) P. Pfeiffer and H. Pfitzner, *J. Prakt. Chem.*, **145**, 243 (1936).
(7) C. A. Bear, J. M. Waters, and T. N. Waters, *J. Chem. Soc. A*, 2494 (1970).
(8) D. Y. Jeter and W. E. Hatfield, *Inorg. Chim. Acta*, **6**, 440 (1972).
(9) A. Earnshaw, B. N. Figgis, and J. Lewis, *J. Chem. Soc. A*, 1656 (1966).
(10) G. F. Kokoszka and R. W. Duerst, *Coord. Chem. Rev.*, **5**, 209 (1970).
(11) K. W. H. Stevens, *Proc. R. Soc. London, Ser. A*, **214**, 237 (1952).
(12) The equation gives the maximum zero-field splitting which occurs when the $g_{\|}$ direction is perpendicular to the Cu–Cu vector.
(13) P. S. W. Boyd, A. D. Toy, T. D. Smith, and J. R. Pilbrow, *J. Chem. Soc. Dalton Trans.*, 1549 (1973).
(14) Supplementary material.
(15) A. P. Ginsberg and M. E. Lines, *Inorg. Chem.*, **11**, 2289 (1972).
(16) F. Lions and K. V. Martin, *J. Am. Chem. Soc.*, **79**, 1273 (1957).
(17) T. P. Cheeseman, D. Hall, and T. N. Waters, *J. Chem. Soc. A*, 1396 (1966).
(18) P. J. Hay, J. C. Thibeault, and R. Hoffmann, *J. Am. Chem. Soc.*, **97**, 4884 (1975).
(19) C. K. Jargenson, "Modern Aspects of Ligand Field Theory", North Holland Publishing Co., Amsterdam, 1971, pp 317, 318.
(20) R. W. Jotham and S. F. A. Kettle, *Inorg. Chem.*, **9**, 1390 (1970).
(21) A. P. Ginsberg, R. L. Martin, R. W. Brookes, and R. C. Sherwood, *Inorg. Chem.*, **11**, 2884 (1972).
(22) P. W. Ball and A. B. Blake, *J. Chem. Soc. A*, 1415 (1969); *J. Chem. Soc. Dalton Trans.*, 852 (1974).
(23) D. M. Duggan and D. N. Hendrickson, *Inorg. Chem.*, **14**, 1944 (1975).
(24) H. M. L. Dieteren and C. Konigsberger, *Recl. Trav. Chim. Pays-Bas*, **82**, 5 (1963); D. Lloyd and R. H. McDougall, *J. Chem. Soc.*, 4136 (1960).
(25) C. G. Pierpont, L. C. Francesconi, and D. N. Hendrickson, *Inorg. Chem.*, **16**, 2367 (1977).

Contribution from the School of Chemical Sciences and the Materials Research Laboratory, University of Illinois, Urbana, Illinois 61801

EPR and Magnetic Susceptibility Studies of the Trinuclear Complex Cyanuratotris[bis(η^5-methylcyclopentadienyl)titanium(III)], the Binuclear Complex Uracilatobis[bis(η^5-methylcyclopentadienyl)titanium(III)], and Related Compounds

BENJAMIN F. FIESELMANN,[1] DAVID N. HENDRICKSON,*[2] and GALEN D. STUCKY*[1]

Received February 8, 1978

The first reported paramagnetic titanium(III) trinuclear compounds, cyanuratotris[bis(η^5-cyclopentadienyl)titanium(III)] (**3**) and cyanuratotris[bis(η^5-methylcyclopentadienyl)titanium(III)] (**4**), were prepared. The structurally related mononuclear compound bis(η^5-cyclopentadienyl)(2-hydroxypyridinato)titanium(III) (**1**) and binuclear compound uracilatobis[bis(η^5-methylcyclopentadienyl)titanium(III)] (**2**) were also synthesized in order to investigate the magnetic exchange interaction between the paramagnetic metal centers. All the compounds are thermally stable and melt without decomposition at over 100 °C. They are also air sensitive. The susceptibility of cyanuratotris[bis(η^5-methylcyclopentadienyl)titanium(III)] shows the presence of an antiferromagnetic interaction at temperatures below 10 K with a J value of -0.93 cm^{-1}. The EPR spectrum of this trinuclear species in a glass at 77 K is that expected for thermal population of both the quartet ($S = {}^3/_2$) and the two doublet ($S = {}^1/_2$) states. The two Ti(III) ions in the dimer, uracilatobis[bis(η^5-methylcyclopentadienyl)titanium(III)], are weakly antiferromagnetically coupled with a J value of -2.25 cm^{-1}. The EPR spectrum of the dimer in a glass at 77 K is that of a triplet system ($S = 1$) with zero field splitting. The six $\Delta M_s = 1$ resonances can be fit to the theoretical equations to give $|D| = 0.0117$ (4) cm^{-1} and $|E| = 0.0018$ (4) cm^{-1}. The similarity in J values for the binuclear and trinuclear molecules suggests that related magnetic exchange pathways are operative.

Introduction

Magnetic exchange interactions have been reported for trinuclear paramagnetic complexes of Cr(III),[3] Fe(III),[4] Ni(II),[5] and Cu(II).[6] Because most of these trinuclear complexes are either insoluble or dissociate in solution, the characterization has been limited largely to magnetic studies on polycrystalline powders. The EPR spectra for these powders generally provide little information due to poor resolution. One exception is the trinuclear vanadyl pyrophosphate complex, $Na_6(VOP_2O_7)_3 \cdot 12H_2O$, which exhibits a 22-line hyperfine spectrum in aqueous solution.[7] On the other hand, several organic triradicals have been studied with EPR. The organic triradicals, of course, also display magnetic exchange interactions, but the magnitude of the exchange

0020-1669/78/1317-1841$01.00/0